

Received Date : 03-Jan-2013  
Revised Date : 07-May-2013  
Accepted Date : 28-May-2013  
Article type : Research Article

## **Rationally Designed Sulfamides As Glutamate Carboxypeptidase II (GCPII) Inhibitors**

Cindy J. Choy,<sup>a</sup> Melody D. Fulton,<sup>a</sup> Austen L. Davis,<sup>a</sup> Mark Hopkins,<sup>a</sup> Joseph K. Choi,<sup>a</sup>  
Marc O. Anderson,<sup>b</sup> Clifford E. Berkman<sup>a,\*</sup>

<sup>a</sup>*Department of Chemistry, Washington State University, Pullman, WA 99164-4630*

<sup>b</sup>*Department of Chemistry and Biochemistry, San Francisco State University,  
San Francisco, CA 94132*

\*Tel 509-335-7613, Fax 509-335-8867, cberkman@wsu.edu

**Keywords:** glutamate carboxypeptidase II, GCP2, prostate specific membrane antigen, PSMA, sulfamide.

### **Abstract**

Glutamate carboxypeptidase II (GCPII) is a membrane-bound cell-surface peptidase. There is significant interest in the inhibition of GCPII as a means of neuroprotection, while GCPII inhibition as a method to treat prostate cancer remains a topic of further investigation. The key zinc-binding functional group of the well-characterized classes of GCPII inhibitors (phosphonates and phosphoramidates) is tetrahedral and negatively charged at neutral pH, while glutamyl urea class of inhibitors possess a planar and neutral zinc-binding group. This current study explores a new class of GCPII inhibitors, glutamyl sulfamides, which possess a putative net neutral

This article has been accepted for publication and undergone full peer review but has not been through the copyediting, typesetting, pagination and proofreading process which may lead to differences between this version and the Version of Record. Please cite this article as an

'Accepted Article', doi: 10.1111/cbdd.12174

This article is protected by copyright. All rights reserved.

tetrahedral zinc-binding motif. A small library containing 6 sulfamides was prepared and evaluated for inhibitory potency against purified GCPII in an enzymatic assay. While most inhibitors have potencies in the micromolar range, one showed promising sub-micromolar potency, with the optimal inhibitor in this series being aspartyl-glutamyl sulfamide (**2d**). Lastly, computational docking was used to develop a tentative binding model on how the most potent inhibitors interact with the ligand-binding site of GCPII.

## Introduction

The expression of glutamate carboxypeptidase II (GCPII) in human prostate epithelium is known as prostate-specific membrane antigen (PSMA). GCPII is a glycosylated cell surface zinc metallopeptidase overexpressed on prostate cancer cells and neovasculature of non-prostatic malignancies (1, 2). As a consequence, GCPII has attracted significant attention as a target for the delivery of imaging and therapeutic agents and continues to serve as an important biomarker. Several studies have suggested that targeting GCPII with small molecules (3, 4) and monoclonal antibodies (4-6) has potential in the development of therapeutic strategies against prostate cancer. However, the most established use of GCPII inhibitors has been in the diagnostic imaging of prostate cancer (4, 7). In the nervous system, GCPII has been implicated in the critical role of regulating synaptic glutamate levels. The presence of excess glutamate has been implicated in several neurological disorders including ischemia, traumatic brain injury (TBI), stroke, and amyotrophic lateral sclerosis (ALS) (4, 8, 9). One source of glutamate in the nervous system is proteolysis of the short neuropeptide N-acetylaspartylglutamate (NAAG), a reaction catalyzed by GCPII. As such, inhibition of CNS GCPII causes decreased levels of extracellular glutamate (10), as well as also increased levels of NAAG which itself has a neuroprotective role (11). Therefore there is significant interest in the inhibition of GCPII as a means of neuroprotection.

Of the known classes of GCPII inhibitor scaffolds, they are typically characterized by a zinc-binding group connected to either a glutaryl or the glutamyl group, which generally serves as the C-terminal or P1' residue of the chemical scaffold (4, 8). For most of these inhibitors, the glutarate/glutamate residue appears to occupy the S1'

pocket of GCPII (12, 13), while additional motifs (if present) occupy the S1 pocket. Key classes of inhibitors (**Figure 1**) include: phosphonates (**1a**), phosphates (**1b**), phosphoramidates (**1c-1e**), and ureas (**1f**) (4, 8). In the case of the phosphorous-based inhibitors, the phosphoryl functionality appears to serve as zinc binding group (ZBG) to the co-catalytic zinc atoms in the active site (12, 13). A problem with the highly potent (yet highly charged) phosphonate inhibitor 2-PMPA (**1a**) and other phosphorous-based inhibitors is their poor oral bioavailability (14) and high renal clearance (15) thereby potentially limiting their practical value as clinical therapeutic agents.

One of our goals is to identify alternative functional groups that could serve as a ZBG group to interact with the co-catalytic zinc atoms in GCPII. In addition, it is expected that these functional groups could also passively serve as a linker between P1-glutamate and a P1' residue to achieve favorable contacts in the active site of GCPII. One attractive scaffold is the glutamyl urea, pioneered by Kozikowski et al (4), and has been co-crystallized with GCPII (16). Recent structural investigation shows the urea oxygen of these inhibitors is approximately 1 Å further away from the catalytic zinc atoms (compared to the tetrahedral phosphonate moiety), but additional interactions in the S1 pocket compensate for the weak binding of the urea group to the active site zinc atoms (16). Another attractive putative zinc-binding motif is the tetrahedral sulfonamide and sulfamide, which allows for trivial installation into small molecule inhibitors. Both the sulfonamide and sulfamide moieties are desirable for pharmaceutical development, compared to similar phosphorous-based groups (**1a-1e**) due to their aqueous stability and their net neutral charge. Short alkyl sulfonamides have showed promise as GCPII inhibitors (17). Although not always functioning as a ZBG, the sulfamide motif has been employed in the design of biologically active agents against various classes of enzymes such as aspartic proteases (18, 19) (HIV-1 protease, gamma-secretase), serine proteases (20) (elastase, chymase, tryptase and thrombin), and metalloproteinase (21) (carboxypeptidase A [CPA] and matrix metalloproteinases [MMPs]). One biochemical target for which sulfamides have been successfully used as a zinc-binding groups is CPA, where single-crystal X-ray diffraction reveals that the sulfamoyl moiety interacts with the active site zinc ion (21). An important feature of sulfamides (as well as ureas

and sulfonamides) is the ease in which they can be conjugated to chiral and inexpensive protected glutamate building blocks (**8** or **9**) to generate an optically active inhibitor scaffold. In contrast, the highly potent phosphonate inhibitors (e.g. 2-PMPA) are more challenging to produce in optically active form (22).

The focus of this study was aimed at (1) the development of a facile synthetic methodology; (2) utilization of methodology to generate a small library of simple glutamyl sulfamides; (3) modeling of a potential binding mode using computational docking.

## RESULTS AND DISCUSSION

A simple method, amenable to parallel synthesis, was employed to synthesize the sulfamide inhibitor library (**Scheme 1**). The common oxazolidinone intermediate and sulfamides were synthesized as outlined by Borghese and coworkers with minor modifications (23). Briefly, commercially available chlorosulfonyl isocyanate was treated with 2-bromoethanol or benzyl alcohol, followed by treatment with di-protected glutamic acid (**8** or **9**) to generate the oxazolidinone intermediates **4** or **5** and Cbz-glutamyl sulfamide **7** respectively. Nucleophilic displacement of the oxazolidinone in **4** or **5** was carried out with amines **6a-e** to generate methyl and benzyl protected sulfamides **3a-e**. Amines **6a**, **6a'**, and **6d-e** could be purchased, while **6b-c** were prepared in two steps from commercially available amino acid precursors by coupling to form the benzamide followed by *tert*-butyl ester deprotection (see supporting information). Last, **3b-e** were deprotected by either ester hydrolysis or hydrogenolysis to form inhibitor candidates **2b-2e**, while **3a** and **3a'** required additional elaboration.

The synthesis of the urea analog **2a** and its diastereomeric partner **2a'** required the installation of the *p*-iodo-phenyl urea moiety at the  $\epsilon$ -amino group prior to global deprotection procedures (**Scheme 2**). The Cbz group from **3a** was selectively removed under catalytic transfer hydrogenolysis conditions to generate the free amine. After overnight drying *in vacuo*, the amine was treated with *p*-iodo-phenyl isocyanate and TEA in DCM to yield **10a**, which was subsequently subjected to global deprotection to yield the target compound **2a**. The diastereomeric partner **2a'** was prepared analogously from **3a'**.

Applying the methodology described in **Schemes 1-2**, a library of potential GCPII inhibitors containing a sulfamide moiety was prepared. The objective of the library design was to test whether the sulfamide core can serve as a ZBG or passively serve as a bridging unit to connect moieties spanning the S1 and S1' regions of the active-site. We generated 2-(sulfamoylamino)pentanedioic acid (**2f**) to test whether the terminal sulfamide can serve as a PSMA inhibitor via interaction with the co-catalytic zincs. In addition, we generated structural analogs of known GCPII inhibitors to test whether the sulfamide core can serve as a linking unit.

Once prepared, the sulfamide inhibitors **2a-f** were assayed for inhibition against purified GCPII with results indicated as 50% inhibitory concentration ( $IC_{50}$ ) values (**Table 1**) (24). Based on previous reports, the sulfamide moiety is capable of interacting with the active site Zn in other zinc metalloproteases such as CPA (21) and carbonic anhydrase (25). Therefore, we hypothesized that sulfamide motif in compound **2f** would act as a ZBG and exhibit greater inhibitory potency than glutamate alone (428  $\mu$ M) (12). Upon comparing the potency of **2f** to that of **1c** ( $IC_{50} = 0.86$  nM) (26) against GCPII, it was concluded that either the sulfamide motif in **2f** is not interacting with the active site Zn or that the interaction with the Zn cation is weak.

The non-classical isosteric replacement of the urea group by the sulfamide motif in a known GCPII inhibitor **1f** ( $IC_{50}=20$  nM) (27) also resulted in sulfamide analog **2a** and its diastereomeric partner **2a'** albeit with decreased inhibitory potency. We hypothesized that the observed poor potency in the diastereomeric pairs could be due to; 1) the weak zinc interaction of the sulfamide moiety; or 2) lack of functionality capable of interacting with the arginine patch. The P1  $\alpha$ -carboxylate in the parent urea inhibitor (**1f**) makes favorable interactions with Asn519, as well as residues Arg534 and Arg536 of the arginine patch (16). Reorientation of this carboxylate due to the presence of the tetrahedral sulfamide group may prevent the favorable interactions of the P1  $\alpha$ -carboxylate present in **2a-2a'** with these Asn and Arg residues, resulting in decreased affinity. This led us to conclude the non-classical isosteric replacement of the known urea GCPII inhibitor was detrimental and resulted in loss of potency.

To obtain better understanding of the sulfamide core as a putative ZBG and its interactions with the active site, we have included **2b** in our library design considerations. Because it is a direct structural analog of a known pseudoirreversible GCPII inhibitor **1e** (IC<sub>50</sub>=35 nM) (26), it allowed for an interrogation of the sulfamide as a isostere of the phosphoramidate group. Despite preserving the tetrahedral geometry of a phosphoramidate as well as features of the P1 and P1' functionality, this isosteric replacement resulted in a considerable loss of inhibitory potency towards GCPII, presumably due to incompatibility of the sulfamide center as a ZBG.

Based on the above observations, we introduced greater flexibility in our inhibitor design in the P1 residue to promote additional interactions with the well-known hydrophobic pocket and arginine patch proximal to the active site. Compounds **2d** and **2e** were designed to allow a carboxylate to probe the arginine patch and/or potentially chelate to the active site Zn, while compound **2c** was introduced to probe for hydrophobic binding interactions. In general, by introducing greater flexibility, the inhibitory potencies of **2c-e** improved.

To shed light on the mode of binding of the more potent sulfamides in this study, computational docking was performed on compounds **2d**, **2e**, and **2f** using a high-resolution X-ray crystal structure of GCPII (pdb = 3D7H), co-crystallized with urea inhibitor DCIBzL (16), using the software FRED (OpenEye Scientific, Santa Fe, NM)(28, 29). Docking was performed in the absence of a pharmacophore restraint. A summary of the docking results of **2d** and **2e** are presented in **Figure 2**, and rendered images are provided in **Figures S1-S2** (Supporting Information). Un-restrained docking of these two inhibitors places them in poses inconsistent with numerous other glutamate containing inhibitors with known modes of binding (**1c**, DCIBzL, etc) which clearly project the P1' Glu  $\gamma$ -carboxylate group into the S1' pocket to form a salt bridge with Lys699, and with the P1'  $\alpha$ -carboxylate interacting with Arg210. In our model of **2d** and **2e**, the P1' Glu  $\gamma$ -carboxylate interacts with the co-catalytic zinc atoms, while the P1'  $\alpha$ -carboxylate interacts with Arg534 and Arg536. In declining affinity for zinc, the order is: histidine > carboxylate > sulfhydryl > phenol > lysine > main chain carbonyl (30),

therefore it is not surprising to see that carboxylate groups replace the sulfamide groups to act as a stronger zinc binder. In these inhibitors, the sulfamide functionality does not appear to be important for binding. In inhibitor **2d**, the P1  $\beta$ -carboxylate interacts with Arg534 and Arg536, while the P1  $\alpha$ -carboxylate interacts with Arg463 and Arg534. The slightly less potent inhibitor **2e** contains an extra methylene group on its side chain; the P1  $\gamma$ -carboxylate interacts with Arg463 and Arg536, while the P1  $\alpha$ -carboxylate is only within distance of interacting with Arg534. In most cases, the interactions are considered to be salt bridges between charged functionality ( $<4 \text{ \AA}$  between the charged atoms) (31), while in some cases, we were able to identify potential hydrogen bonds as well ( $< 3.2 \text{ \AA}$  between the donor and acceptor; angle between HBD-H $\cdots$ HBA  $> 150^\circ$ ) (32). The specific non-covalent interactions, including distances determined in the course of our docking simulations of **2d** and **2e** are presented in **Table S1**. A superimposition of compounds **2d** and **2e** docked into the catalytic site is presented in **Figure S3**, showing a generally consistent mode of binding, aside from the position of the terminal P1 carboxylate groups, due to the longer side chain in **2e**, while the remainder of the two structures are positioned fairly consistently.

The possibility that **2d** and **2e** adopt a novel pose is interesting, and would need to be validated by a more rigorous structural method such as X-ray crystallography. To provide evidence against the “classical” mode of binding of these inhibitors (P1' into S1'), we also performed docking of **2d** and **2e** in the presence of a pharmacophore constraint that required the P1'  $\gamma$ -carboxylate to be within  $3.5 \text{ \AA}$  of Lys699 in the S1' pocket, allowing the compounds to dock in a manner more consistent with other GCP II inhibitors (data not presented). While such poses would be appealing in that they share consistency with X-ray crystal structures of phosphorous and urea-based inhibitors, the seven independent scoring functions in FRED score such poses with significantly higher energy than the novel poses presented in **Figure 2**.

Our model does not precisely explain the slightly improved potency of **2d** ( $IC_{50} = 0.9 \text{ \mu M}$ ) versus **2e** ( $IC_{50} = 1.2 \text{ \mu M}$ ), as both compounds make a similar number of contacts (with similar distances) to the residues in the arginine patch. Nevertheless, it

can be noted: (a) while the P1  $\alpha$ -carboxylate in both compounds can obtain salt bridge interactions with Arg463, this carboxylate in **2d** is within distance to make a second salt bridge interaction with Arg534, while this group in **2e** is bent slightly away from Arg534, and less likely to interact; (b) the relative potency of the compounds is within experimental error, thus one must be cautious to conclude **2d** is actually more potent than **2e**.

We also performed un-restrained docking of the less potent inhibitor **2f**, which is a sulfamide analog of the extremely potent and structurally analogous phosphoramidate inhibitor (**1c**) (**Figure S4**). Our model of this compound also changes its orientation from the classical binding mode observed for phosphorous and urea-based inhibitors. In our model of **2f**, one sulfamide S=O group hydrogen bonds with Arg210, while the Glu  $\alpha$ -carboxylate interacts with zinc. The Glu  $\gamma$ -carboxylate interacts with Arg534 and Arg536 through a salt bridge and through hydrogen bonding interactions. While the interactions seem reasonable, caution must be exercised due to the relatively poor potency of this inhibitor ( $IC_{50} = 6 \mu M$ ).

## Conclusion and Future Work

A small library of sulfamide analogs of known GCPII inhibitor scaffolds was prepared to interrogate the value of the sulfamide motif as a zinc-binding group for this and other metallopeptidases. While the majority of the inhibitors were modestly active, one inhibitor (**2d**), which contains an ASP  $\beta$ -carboxylate for the S1 pocket, possessed sub-micromolar activity. Binding modes for three of the more potent compounds (**2d-2f**) was rationalized by a binding model generated by computational docking. Our model suggests that the two most potent compounds (**2d** and **2e**) obtain a non-conventional binding mode, in which the sulfamide group does not interact with the co-catalytic zinc atoms, but with the acidic side chain functionality greatly interacting with the residues in the S1 arginine patch region. The less potent inhibitor **2f** docked in a conformation that suggests the sulfamide oxygens contribute to zinc binding.

Sulfamides that lack both  $\alpha$ - or  $\beta$ -carboxylate in the P1 residue resulted in poor inhibition. Based on the results of our initial sulfamide library, we conclude the sulfamide moiety is not a good zinc binding group for GCPII (in contrast with other proteins like CPA).

## Materials and Methods

***IC<sub>50</sub> Determinations for GCPII Inhibition.*** Inhibitions studies were performed as previously described (17, 33, 34).

***Synthesis.*** All solvents used in reactions were both anhydrous and obtained from commercial sources. <sup>1</sup>H and <sup>13</sup>C NMR spectra were recorded on a Bruker 400 MHz spectrometer or a Varian 300 MHz. <sup>1</sup>H NMR chemical shifts are relative to TMS ( $\delta=0.00$  ppm), CDCl<sub>3</sub> ( $\delta=7.26$  ppm), CD<sub>3</sub>OD ( $\delta=3.31$  ppm) or D<sub>2</sub>O ( $\delta=4.79$  ppm). <sup>13</sup>C NMR chemical shifts are relative to CDCl<sub>3</sub> ( $\delta=77.23$  ppm), CD<sub>3</sub>OD ( $\delta=49.00$  ppm). Mass spectrometry spectra were obtained on an Applied Biosystems 4800 MALDI- TOF/TOF mass spectrometer.

*General procedure for oxazolidinone-glutamyl sulfamide preparation (4 and 5).* To a solution of chlorosulfonyl isocyanate (1.538 mL, 17.66 mmol) at 0°C in DCM (7 mL), was added a solution of 2-bromoethanol (1.26 mL, 17.78 mmol) in DCM (10 mL) slowly via addition funnel and maintain reaction temperature range of 0-5°C. Upon complete addition, the reaction was stirred for an hour at 0-5°C, followed by the addition of **8** or **9** (19.43 mmol) in DCM (18 mL) and TEA (7.87 mL, 56.52 mmol). The solution was added slowly to maintain reaction temp 0-5°C. Once addition was complete, the resulting reaction mixture was allowed to warm to RT and stirred overnight. After overnight stirring, the reaction mixture was washed with 1N HCl (2X, 50 mL) followed by brine (50 mL). Water was added to the organic layer and DCM was evaporated to yield a precipitate (70-86%) and further used without purification.

*(S)-dimethyl 2-(2-oxooxazolidine-3-sulfonamido)pentanedioate (4):* (85.6%) <sup>1</sup>H NMR (400 MHz, DMSO-d<sub>6</sub>)  $\delta$  9.08 (d,  $J = 9.0$  Hz, 1H), 4.43-4.25 (m, 2H), 4.12 (td,  $J = 9.5, 4.7$  Hz, 1H), 3.97-3.83 (m, 2H), 3.67 (s, 3H), 3.57 (s, 3H), 2.43-2.34 (m, 2H), 2.04-

1.96 (m, 1H), 1.78-1.69 (m, 1H). <sup>13</sup>C NMR (100 MHz, DMSO-d6) δ 172.86, 171.86, 153.18, 62.88, 55.64, 52.89, 51.88, 45.77, 29.65, 27.09.

(*S*)-dibenzyl 2-(2-oxooxazolidine-3-sulfonamido)pentanedioate (**5**): (69.8%) <sup>1</sup>H NMR (400 MHz, DMSO-d6) δ 9.14 (d, *J* = 8.8 Hz, 1H), 7.49-7.14 (m, 10H), 5.25-4.92 (m, 4H), 4.37-4.12 (m, 3H), 4.01-3.67 (m, 2H), 2.46-2.35 (m, 2H), 2.08-2.00 (m, 1H), 1.83-1.74 (m, 1H). <sup>13</sup>C NMR (100 MHz, DMSO-d6) δ 172.27, 171.37, 153.16, 136.48, 135.98, 128.87, 128.85, 128.62, 128.45, 128.40, 128.38, 67.08, 66.05, 62.85, 55.79, 45.75, 29.85, 27.18.

*General procedure for methyl ester deprotection.*(**2a**, **2a'**, **2b**, and **2c**). To a solution of **3a-c** in 1,4-Dioxane (1 mL), was added 1 M LiOH (1.5 eq/methyl ester). The resulting solution was stirred at room temperature until completion. Upon completion, the reaction mixture was acidified (pH=3) with 4 M HCl. The organic solvent was removed and the crude mixture was taken up to 0.5 mL with HPLC grade methanol, micro filtered then peak purified with a preparative Thermo Scientific\* Hypersil\* GOLD preparative C18 column (20mm x 50mm, particle size 5 um) running a 5% to 97% gradient of water/methanol with 0.1% formic acid with a 15 mL/min flow rate on a SpectraSystem HPLC. Chromatographs were monitored with single wavelength UV detector at 254 nm. Fractions were concentrated down to yield a white solid (57-65%).

(*2S*)-2-((*N*-(1-carboxy-5-(3-(4-iodophenyl)ureido)pentyl)sulfamoyl)amino)pentanedioic acid (**2a**): (65.4%) <sup>1</sup>H NMR (400 MHz, CD<sub>3</sub>OD) δ 7.52 (d, *J* = 8.8 Hz, 1H), 7.17 (d, *J* = 8.7 Hz, 1H), 4.00-3.96 (m, 1H), 3.94-3.91 (m, 1H), 3.18 (t, *J* = 6.5 Hz, 1H), 2.55-2.34 (m, 1H), 2.17-2.10 (m, 1H), 1.98-1.77 (m, 1H), 1.76-1.67 (m, 1H), 1.61-1.38 (m, 2H). <sup>13</sup>C NMR (100 MHz, CD<sub>3</sub>OD) δ 175.06, 174.35, 173.90, 173.55, 156.54, 139.67, 137.28, 120.50, 83.63, 55.53, 54.88, 54.82, 50.75, 39.11, 32.13, 29.37, 29.30, 29.27, 27.69, 27.61, 22.31, 22.28. NMR spectra for **2a'** is identical to **2a**. M/Z calculated for C<sub>18</sub>H<sub>24</sub>IN<sub>4</sub>O<sub>9</sub>S [M-H] 599.0314; found [M-H] 599.0011.

(*S*)-2-((*N*-((*S*)-2-benzamido-2-carboxyethyl)sulfamoyl)amino)pentanedioic acid (**2b**): (58.6%) <sup>1</sup>H NMR (400 MHz, CD<sub>3</sub>OD) δ 7.93-7.85 (m, 2H), 7.61-7.51 (m, 1H), 7.51-7.44 (m, 2H), 4.72-4.69 (m, 1H), 3.96-3.92 (m, 1H), 3.66-3.46 (m, 2H), 2.53-2.41

(m, 2H), 2.19-2.09 (m, 1H), 1.95-1.82 (m, 1H).  $^{13}\text{C}$  NMR (100 MHz,  $\text{CD}_3\text{OD}$ )  $\delta$  176.48, 176.46, 175.53, 175.43, 173.30, 170.12, 170.06, 135.06, 132.93, 129.57, 128.52, 128.51, 56.43, 54.91, 44.69, 31.01, 29.16.  $M/Z$  calculated for  $\text{C}_{15}\text{H}_{18}\text{N}_3\text{O}_9\text{S}$  [M-H] 416.0769; found [M-H] 416.0920.

*(S)*-2-((*N*-((*S*)-3-benzamido-3-carboxypropyl)sulfamoyl)amino)pentanedioic acid (**2c**): (57.2%)  $^1\text{H}$  NMR (400 MHz,  $\text{CD}_3\text{OD}$ )  $\delta$  7.91-7.82 (m, 2H), 7.57-7.50 (m, 1H), 7.50-7.41 (m, 2H), 4.67-4.62 (m, 1H), 3.92-3.88 (m, 1H), 3.23-3.02 (m, 2H), 2.50-2.39 (m, 2H), 2.28-2.16 (m, 1H), 2.15-1.94 (m, 1H), 1.92-1.79 (m, 1H).  $^{13}\text{C}$  NMR (100 MHz,  $\text{CD}_3\text{OD}$ )  $\delta$  175.00, 174.31, 173.82, 169.05, 133.77, 131.41, 128.09, 127.14, 127.13, 54.94, 50.83, 39.49, 30.98, 29.56, 27.71, 27.69.  $M/Z$  calculated for  $\text{C}_{16}\text{H}_{20}\text{N}_3\text{O}_9\text{S}$  [M-H] 430.0926; found [M-H] 430.0882.

*General procedure for hydrogenolysis (2d, 2e, and 2f)*. Ammonium formate (5 eq/benzyl ester) was added to a rapidly stirred suspension of **3d-f**, Pd/C (0.03 eq) and potassium bicarbonate (1.0 eq/carboxylate) in 1,4-Dioxane: water solution (2:1 v/v, 2 mL). The reaction was stirred until completion. Upon completion, the reaction mixture was filtered and concentrated down to produce the desired compound in quantitative yield as the potassium salt.

*(S)*-2-((*N*-((*S*)-1,2-dicarboxyethyl)sulfamoyl)amino)pentanedioic acid (**2d**): (95.3%)  $^1\text{H}$  NMR (400 MHz,  $\text{D}_2\text{O}$ )  $\delta$  3.82-3.75 (m, 1H), 3.55-3.48 (m, 1H), 2.50-2.39 (m, 1H), 2.35-2.20 (m, 1H), 2.10-1.96 (m, 2H), 1.82-1.60 (m, 2H).  $^{13}\text{C}$  NMR (100 MHz,  $\text{D}_2\text{O}$ )  $\delta$  182.20, 179.28, 178.86, 178.48, 58.00, 57.97, 56.11, 56.01, 40.68, 33.69, 33.59, 29.24, 29.20.  $M/Z$  calculated for  $\text{C}_9\text{H}_{13}\text{N}_2\text{O}_{10}\text{S}$  [M-H] 341.0296; found [M-H] 340.8914.

*(2S,2'S)*-2,2'-(sulfonylbis(azanediyl))dipentanedioic acid (**2e**): (97.3%)  $^1\text{H}$  NMR (400 MHz,  $\text{D}_2\text{O}$ )  $\delta$  3.72-3.55 (m, 2H), 2.29-2.13 (m, 4H), 2.01-1.73 (m, 4H).  $^{13}\text{C}$  NMR (100 MHz,  $\text{D}_2\text{O}$ )  $\delta$  182.08, 179.20, 58.07, 33.73, 29.28.  $M/Z$  calculated for  $\text{C}_{10}\text{H}_{15}\text{N}_2\text{O}_{10}\text{S}$  [M-H] 355.0453; found [M-H] 355.0450.

*(S)*-2-(sulfamoylamino)pentanedioate (**2f**): (100%)  $^1\text{H}$  NMR (400 MHz, Deuterium Oxide)  $\delta$  3.74 (td,  $J = 8.5, 5.0$  Hz, 1H), 2.42-2.28 (m, 2H), 2.10-1.95 (m, 1H), 1.88-1.79

(m, 1H).  $^{13}\text{C}$  NMR (100 MHz,  $\text{D}_2\text{O}$ )  $\delta$  180.01, 178.68, 170.50, 62.38, 57.75, 31.97, 28.46. M/Z calculated for  $\text{C}_5\text{H}_9\text{N}_2\text{O}_6\text{S}$  [M-H] 225.0187; found [M-H] 225.0301.

## References and Notes

1. Haffner MC, Kronberger IE, Ross JS, Sheehan CE, Zitt M, Muhlmann G, et al. Prostate-specific membrane antigen expression in the neovasculature of gastric and colorectal cancers. *Hum Pathol.* 2009;40(12):1754-61. Epub 2009/09/01.
2. Chang SS, O'Keefe DS, Bacich DJ, Reuter VE, Heston WD, Gaudin PB. Prostate-specific membrane antigen is produced in tumor-associated neovasculature. *Clinical cancer research : an official journal of the American Association for Cancer Research.* 1999;5(10):2674-81.
3. Tang H, Brown M, Ye Y, Huang G, Zhang Y, Wang Y, et al. Prostate targeting ligands based on N-acetylated alpha-linked acidic dipeptidase. *Biochem Biophys Res Commun.* 2003;307(1):8-14.
4. Zhou J, Neale JH, Pomper MG, Kozikowski AP. NAAG peptidase inhibitors and their potential for diagnosis and therapy. *Nat Rev Drug Discov.* 2005;4(12):1015-26.
5. Chang SS. Monoclonal antibodies and prostate-specific membrane antigen. *Curr Opin Investig Drugs.* 2004;5(6):611-5.
6. Chang SS. Overview of prostate-specific membrane antigen. *Rev Urol.* 2004;6 Suppl 10:S13-8. Epub 2006/09/21.
7. Bander NH. Technology insight: monoclonal antibody imaging of prostate cancer. *Nature clinical practice.* 2006;3(4):216-25.
8. Tsukamoto T, Wozniak KM, Slusher BS. Progress in the discovery and development of glutamate carboxypeptidase II inhibitors. *Drug Discov Today.* 2007;12(17-18):767-76.
9. Whelan J. NAALADase inhibitors: A novel approach to glutamate regulation. *Drug Discov Today.* 2000;5(5):171-2. Epub 2000/05/02.
10. Vornov JJ, Wozniak K, Lu M, Jackson P, Tsukamoto T, Wang E, et al. Blockade of NAALADase: a novel neuroprotective strategy based on limiting glutamate and elevating NAAG. *Ann N Y Acad Sci.* 1999;890:400-5. Epub 2000/02/11.
11. Kamiya H, Shinozaki H, Yamamoto C. Activation of metabotropic glutamate receptor type 2/3 suppresses transmission at rat hippocampal mossy fibre synapses. *J Physiol.* 1996;493 ( Pt 2):447-55. Epub 1996/06/01.
12. Barinka C, Rovenska M, Mlcochova P, Hlouchova K, Plechanovova A, Majer P, et al. Structural insight into the pharmacophore pocket of human glutamate carboxypeptidase II. *J Med Chem.* 2007;50(14):3267-73.
13. Mesters JR, Henning K, Hilgenfeld R. Human glutamate carboxypeptidase II inhibition: structures of GCPII in complex with two potent inhibitors, quisqualate and 2-PMPA. *Acta Crystallogr D Biol Crystallogr.* 2007;63(Pt 4):508-13.
14. Peng XQ, Li J, Gardner EL, Ashby CR, Jr., Thomas A, Wozniak K, et al. Oral administration of the NAALADase inhibitor GPI-5693 attenuates cocaine-induced

- reinstatement of drug-seeking behavior in rats. *European journal of pharmacology*.627(1-3):156-61.
15. Lapi SE, Wahnische H, Pham D, Wu LY, Nedrow-Byers JR, Liu T, et al. Assessment of an <sup>18</sup>F-labeled phosphoramidate peptidomimetic as a new prostate-specific membrane antigen-targeted imaging agent for prostate cancer. *J Nucl Med*. 2009;50(12):2042-8. Epub 2009/11/17.
  16. Barinka C, Byun Y, Dusich CL, Banerjee SR, Chen Y, Castanares M, et al. Interactions between human glutamate carboxypeptidase II and urea-based inhibitors: structural characterization. *J Med Chem*. 2008;51(24):7737-43. Epub 2008/12/05.
  17. Blank BR, Alayoglu P, Engen W, Choi JK, Berkman CE, Anderson MO. N-substituted glutamyl sulfonamides as inhibitors of glutamate carboxypeptidase II (GCP2). *Chem Biol Drug Des*. 2011;77(4):241-7. Epub 2011/01/12.
  18. Backbro K, Lowgren S, Osterlund K, Atepo J, Unge T, Hulten J, et al. Unexpected binding mode of a cyclic sulfamide HIV-1 protease inhibitor. *J Med Chem*. 1997;40(6):898-902. Epub 1997/03/14.
  19. Sparey T, Beher D, Best J, Biba M, Castro JL, Clarke E, et al. Cyclic sulfamide gamma-secretase inhibitors. *Bioorg Med Chem Lett*. 2005;15(19):4212-6. Epub 2005/08/02.
  20. Zhong J, Gan X, Alliston KR, Lai Z, Yu H, Groutas CS, et al. Potential protease inhibitors based on a functionalized cyclic sulfamide scaffold. *J Comb Chem*. 2004;6(4):556-63. Epub 2004/07/13.
  21. Park JD, Kim DH, Kim SJ, Woo JR, Ryu SE. Sulfamide-based inhibitors for carboxypeptidase A. Novel type transition state analogue inhibitors for zinc proteases. *J Med Chem*. 2002;45(24):5295-302. Epub 2002/11/15.
  22. Vitharana D, France JE, Scarpetti D, Bonneville GW, Majer P, Tsukamoto T. Synthesis and biological evaluation of (R)- and (S)-2-(phosphonomethyl)pentanedioic acids as inhibitors of glutamate carboxypeptidase II. *Tetrahedron: Asymmetry*. 2002;13(15):1609-14.
  23. Borghese A, Antoine L, Van Hoeck JP, Mockel A, Merschaert A. Mild and safer preparative method for nonsymmetrical sulfamides via N-sulfamoyloxazolidinone derivatives: Electronic effects affect the transsulfamoylation reactivity. *Organic Process Research & Development*. 2006;10(4):770-5.
  24. Wu LY, Anderson MO, Toriyabe Y, Maung J, Campbell TY, Tajon C, et al. The molecular pruning of a phosphoramidate peptidomimetic inhibitor of prostate-specific membrane antigen. *Bioorg Med Chem*. 2007;15(23):7434-43.
  25. Abbate F, Supuran CT, Scozzafava A, Orioli P, Stubbs MT, Klebe G. Nonaromatic sulfonamide group as an ideal anchor for potent human carbonic anhydrase inhibitors: role of hydrogen-bonding networks in ligand binding and drug design. *J Med Chem*. 2002;45(17):3583-7. Epub 2002/08/09.
  26. Liu T, Toriyabe Y, Kazak M, Berkman CE. Pseudoirreversible Inhibition of Prostate-Specific Membrane Antigen by Phosphoramidate Peptidomimetics. *Biochemistry*. 2008;47(48):12658-60.
  27. Maresca KP, Hillier SM, Femia FJ, Keith D, Barone C, Joyal JL, et al. A series of halogenated heterodimeric inhibitors of prostate specific membrane antigen

- (PSMA) as radiolabeled probes for targeting prostate cancer. *J Med Chem.* 2009;52(2):347-57. Epub 2008/12/30.
28. McGann M. FRED Pose Prediction and Virtual Screening Accuracy. *Journal of Chemical Information and Modeling.* 2011;51(3):578-96.
  29. McGaughey GB, Sheridan RP, Bayly CI, Culberson JC, Kretsoulas C, Lindsley S, et al. Comparison of topological, shape, and docking methods in virtual screening. *J Chem Inf Model.* 2007;47(4):1504-19. Epub 2007/06/27.
  30. Jaffe EK. Predicting the Zn(II) Ligands in Metalloproteins: Case Study, Porphobilinogen Synthase. *Comments on Inorganic Chemistry.* 1993;15(2):67-92.
  31. Kumar S, Nussinov R. Close-range electrostatic interactions in proteins. *Chembiochem.* 2002;3(7):604-17. Epub 2002/09/27.
  32. Jeffrey GA. An introduction to hydrogen bonding. New York: Oxford University Press; 1997. vii, 303 p. p.
  33. Maung J, Mallari JP, Girtsman TA, Wu LY, Rowley JA, Santiago NM, et al. Probing for a hydrophobic a binding register in prostate-specific membrane antigen with phenylalkylphosphonamidates. *Bioorg Med Chem.* 2004;12(18):4969-79.
  34. Anderson MO, Wu LY, Santiago NM, Moser JM, Rowley JA, Bolstad ES, et al. Substrate specificity of prostate-specific membrane antigen. *Bioorg Med Chem.* 2007;15(21):6678-86.

### Supporting Information

Scheme S1, Figures S1-S3, experimental procedure, and characterization data for intermediates **3a-3e**, and **7**.

**Figure 1.** Known GCPII inhibitors.

**Scheme 1.** Synthesis of glutamyl sulfamides. Reagents and conditions: (a) 2-bromoethanol; (b) benzyl alcohol; (c) HCl.Glu(OMe).OMe (**8**) or Tosyl.Glu(OBn).OBn (**9**); (d) amino acids **6a-e**, TEA, ACN, 50°C; (e) LiOH or Pd/C, NH<sub>4</sub>COOH, KHCO<sub>3</sub>, 1:2 H<sub>2</sub>O:Dioxane (v/v)

**Scheme 2:** Synthesis of sulfamide **2a** and **2a'**. Reagents: (a) Pd/C, NH<sub>4</sub>COOH, KHCO<sub>3</sub>, 1:2 H<sub>2</sub>O:Dioxane (v/v); (b) 4-iodo-phenyl isocyanate, TEA, DCM; (c) LiOH, Dioxane.

**Table 1:** Inhibitory potency of sulfamides against purified GCPII

**Figure 2:** Summary of computational docking results for the most potent compounds **2d** (panel A) and **2e** (panel B) into the active site of an X-ray crystal structure of PSMA (PDB=3D7H). Rendered images are provided in **Figures S1-S2** (Supporting Information).

**Scheme S1.** *Synthesis* of **6b** and **6c**. Reagents and conditions: (a) HBTU, TEA, Benzoic acid, DMF; (b) 4M HCl in Dioxane.

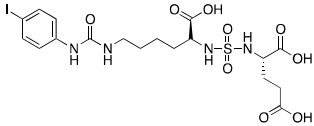
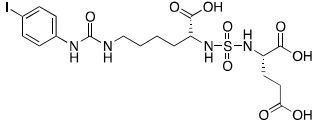
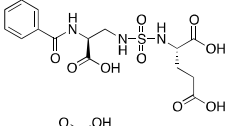
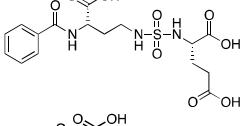
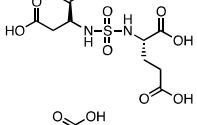
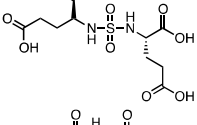
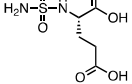
**Figure S1:** Un-restrained computational docking of compound **2d** into the active site of an X-ray crystal structure of GCP2 (PDB=3D7H). The PyMOL Molecular Graphics System (<http://www.pymol.org/>) was used to prepare the molecular drawings.

**Figure S2:** Un-restrained computational docking of compound **2e** into the active site of an X-ray crystal structure of GCP2 (PDB=3D7H).

**Figure S3:** Representation of docked compound **2d** (red) superimposed with **2e** (blue).

**Figure S4:** Un-restrained computational docking of compound **2f** into the active site of an X-ray crystal structure of GCP2 (PDB=3D7H).

**Table S1:** Interactions between ligands 2d-2f, and the GCP2 active site residues, as determined by computational docking. Interaction type: A = salt bridge; B = metal coordination; C = moderate-to-strong hydrogen bond as defined by Jeffrey et al (5). For interactions A-B, the distance is between the associated atoms. For interaction C, the distance is calculated between the hydrogen bond acceptor (typically on the ligand) and a proton on the hydrogen bond donor (in most cases arginine). In most cases, the position of the proton was not shown in **Figures S1-S2** and **S4**, for the purpose of clarity.

Compound	Structure	IC <sub>50</sub> (μM)
2a		5(1)
2a'		10(2)
2b		>100
2c		15(2)
2d		0.9(1)
2e		1.2(1)
2f		5.9(4)

**Table 1:** Inhibitory potency of sulfamides against purified GCPII

